


Experimental Observation of Nonreciprocal Waves in a Resonant Metamaterial Beam

M.A. Attarzadeh¹, J. Callanan¹, and M. Nough^{1*}

Department of Mechanical & Aerospace Engineering, University at Buffalo (SUNY), Buffalo, New York 14260-4400, USA

 (Received 29 October 2019; revised manuscript received 29 December 2019; accepted 27 January 2020; published 14 February 2020)

Space-time-varying materials pledge to deliver nonreciprocal dispersion in linear systems by inducing an artificial momentum bias. Although such a paradigm eliminates the need for actual motion of the medium, experimental realization of space-time structures with dynamically changing material properties has been elusive. In this letter, we present an elastic metamaterial that exploits stiffness variations in an array of geometrically phase-shifted resonators—rather than external material stimulation—to induce a temporal modulation. We experimentally demonstrate that the resulting bias breaks time-reversal symmetry in the resonant metamaterial, and achieves a nonreciprocal tilt of dispersion modes within dynamic modulation regimes.

DOI: [10.1103/PhysRevApplied.13.021001](https://doi.org/10.1103/PhysRevApplied.13.021001)

The ability to control wave propagation in elastic media is of key importance in a number of disciplines that span multiple geometric scales. Resonant and periodic materials aim to provide a means to mitigate or guide elastic waves via precisely engineered periodic variations in structural geometry, allowing wave control features to scale with the structure itself [1–3]. The field of elastic metamaterials possessing unique dispersive features including tunable band gaps, topological edge states, and negative effective properties has received increased attention in recent years [4–7]. Most recently, novel configurations have been presented as pathways to break one of the fundamental elastodynamic principles, *reciprocity*, and onset a diodelike behavior [8–11]. Reciprocity, often used in conjunction with principles of superposition and symmetry, is of key importance for many analysis methods in electromagnetism, acoustics, and signal processing—in practice, however, back scattered waves present a number of issues and limitations in sensing, structural fidelity, telecommunication, and defense applications. Therefore, it is of key interest to develop structures that exhibit a robust nonreciprocal-wave-propagation behavior. Linear systems with space-time modulated material fields have been the focus of a number of efforts to investigate wave amplification and nonreciprocity [12,13]. Due to the time dependence of their properties, these systems are no longer bound by the reciprocity [14], while their response remains amplitude independent, unlike nonlinear counterparts. The

theoretical problem of characterizing elastic wave propagation in space-time modulated systems has been investigated in one- [15] and two-dimensional [16] structures using plane-wave expansion. Recently, this approach has been further extended to discretely modulated structures to better adapt with practical situations [17]. Nonreciprocal waves have also been witnessed in locally resonant systems [18,19] and elastic metamaterial beams [20]. Nonetheless, the realization of time-modulated elastic systems remains a practical challenge due to their dynamic nature. A select number of efforts have conceived ways to realize nonreciprocal media. These include photoelasticity [6], magnetoelastic effects [21–23], piezoelectric materials [24–26], geometric nonlinearity [27,28], and gyroscopic action via angular momentum modulations [29]. Band-gap tunability observed in granular materials with dielectric properties also provides promising avenues to break reciprocity [30,31].

In this work, we present an apparatus that achieves space-time modulation of elastic stiffness in a subwavelength configuration that does not involve smart or adaptive materials with interphysical couplings. The system, which is designed and constructed using widely available components and manufacturing techniques, comprises an elastic metamaterial beam (or metabeam, for short) and relies on local resonators that dynamically vary their effective stiffness by changing their angular orientation with respect to the vibration direction. Such a behavior has been recently used to tune locally resonant band gaps [32]. In addition to breaking wave-propagation symmetry, the proposed design inherits the tunability of frequency band gaps in conventional metamaterials, which in turn

*mnough@buffalo.edu

extends the nonreciprocal behavior to low frequencies. The nonreciprocal metabeam is conceptually akin to a locally resonant metamaterial as depicted in Fig. 1(a) and its well-established dynamics [33,34]. The spring stiffness in each resonator, however, is varied independently in time, and by controlling the macroscopic spatial distribution of the resonators' stiffness, a space-time traveling profile is achieved. Figure 1(b) shows an example of the necessary effective stiffness variation to create nonreciprocity; the stiffness $k(x, t)$ is plotted for two time instants, t_1 and t_2 . The curve $k(x, t_2)$ is identical to $k(x, t_1)$ except for a spatial phase shift. The means of achieving this stiffness variation are of paramount importance for both research and practical implementation purposes. Considering a beam with rectangular cross section (hereafter referred to as resonator arm) as the spring member, as shown in Fig. 1(c), the lateral stiffness under Euler-Bernoulli theory is given by $k = 3EI_x/l^3$, where E is the elastic modulus, l is the arm length, and I_x is the second area moment of arm cross section calculated perpendicular to the vibration direction. We propose that the stiffness variation can be achieved by making use of the second area moment of the resonator arm instead of controlling its elastic modulus E . For a resonator rotated by the angle θ , the value of I_x can be computed by using the principle axes values and a coordinate rotation: let x' and y' be the principle axes for one resonator arm; the relevant moment of area for vibration in the y direction as depicted in Fig. 1(c) is $I_x = I_0 + I_1 \cos(2\theta)$, where $I_0 = \frac{1}{2}(I_{x'} + I_{y'})$ and $I_1 = \frac{1}{2}(I_{x'} - I_{y'})$. Note that the difference in magnitude between the two principle moments is responsible for the alternating variation of I_x and in turn the variation in the resonator stiffness. A series of finite-element numerical simulations are carried out to verify the change in stiffness as a result of the resonator angular rotation. Figure 1(e) shows the stiffness variation with

respect to the angular orientation for rectangular cross sections with aspect ratios $r = 0.25, 0.5, 0.9$, and 1 . Figure 1(e) confirms that a lower aspect ratio results in a greater variation in the arm stiffness as it rotates; the stiffness variation starts deviating from a perfect harmonic variation due to violation of Euler-Bernoulli beam assumptions at lower aspect ratios. The dependence of band gaps on resonator orientation is shown in the literature [32] and confirmed by studying the metamaterial in two different nonrotating configurations, as depicted in Fig. 2. Dispersion diagrams and the corresponding transmission spectra confirm that energy propagation in the metabeam can be dramatically altered by changing only the orientation of the resonators by 90° to switch from the lowest to the highest stiffness configurations (a band gap shift of nearly 400 Hz). Matching experimental results, obtained from the setup outlined in the subsequent section, are also provided. The host beam in Fig. 1(c) is of length L , width W and height H , and is equipped with a series of local resonators that each consist of a prismatic arm with dimensions a, b and l , and a tip mass with a radius R_r and a height H_r . Figure 1(d) shows the angular orientation of the resonators in one unit cell in a metabeam with spatially modulated resonator stiffness. Each resonator is rotated by 45° relative to the previous one such that a repeating unit cell is made up of four local resonators. Let the index j denote a single resonator (more specifically a pair of resonators at the same x location on the beam, top and bottom); a unit cell on the metabeam consists of J resonator pairs. As such, a prescribed phase shift between the resonators angular orientation (45° adjacent resonators) generates a spatial modulation of the stiffness. The space-time modulation of the resonators' stiffness is achieved by a synchronized rotation of the resonators' arms with an angular velocity of ω_p while maintaining the

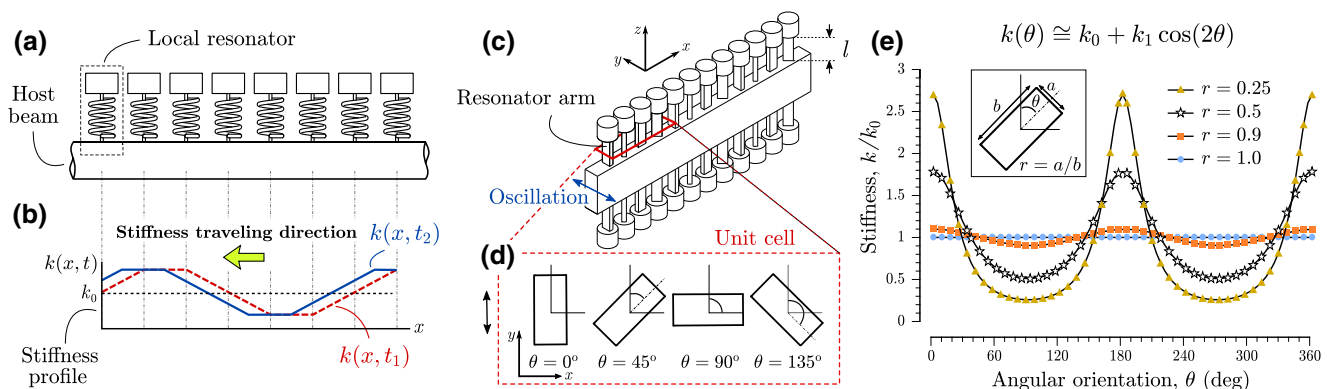


FIG. 1. Schematic representation of the operational principles of the nonreciprocal metabeam: (a) illustration of a conventional metabeam with discretely located resonators; (b) space-time variation of resonators' stiffness traveling in the negative direction of the x axis to induce artificial linear momentum bias; (c) proposed realization of the spatially modulated resonator stiffness in an elastic metabeam; (d) angular orientation of resonators in a unit cell to create the spatial modulation; (e) the stiffness variation of rectangular cross sections with various aspect ratios versus angular orientation.

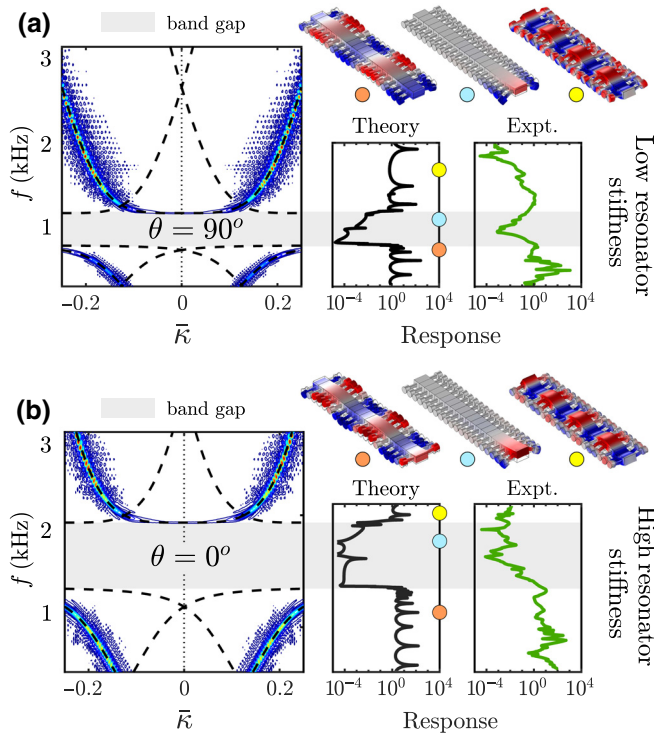


FIG. 2. Dispersion behavior and transmission spectra of the metabeam in two *nonrotating* configurations: (a) low stiffness (all resonators at $\theta = 90^\circ$) and (b) high stiffness ($\theta = 0^\circ$). Shaded regions indicate band gaps. Mode shapes pre, within, and post both band gaps are provided for reference. Metabeam parameters identical to those listed in Fig. 3.

aforementioned spatial modulation. The combined effect of both spatial and temporal variation induces the desired wavelike stiffness pumping. The stiffness of the j th resonator at time t is $k^{(j)}(t) = k_0 + k_1 \cos(\omega_p t + 2\pi j/J)$. The metabeam is constructed following the general operating principles as shown in Fig. 1. The setup consists of the host beam, 40 local resonators grouped into symmetric pairs above and below the beam, and motors to control the resonator angle, along with the measurement and excitation systems, as illustrated in Fig. 3. The metabeam is represented by a black rectangle with the local resonators as circles, similar to a bird's eye view of the actual apparatus, in Fig. 3(g). The stepper motors are controlled with a custom driver array [Fig. 3(d)]. Vibration measurements are taken with a Polytec PSV-500 scanning laser doppler vibrometer (SLDV), illustrated in Fig. 3(b). The temperature of the beam is continuously monitored with a FLIR A325sc thermal imaging camera [Fig. 3(a)] to ensure that the stiffness of the host structure does not vary due to heating or cooling between successive tests. Actuators in the form of two extender piezoelectric plates [and a high-voltage amplifier, Fig. 3(c)] are mounted symmetrically on both sides of the beam and operated 180° out of phase such that transverse vibrations are dominantly excited.

The motors and piezoelectric actuators are directly controlled using LabVIEW and a National Instruments data acquisition system. Further, the SLDV system is triggered using the same controller in order to ensure that the measurements are synchronous with the prescribed temporal modulation of the metabeam. A close-up view of one unit cell in the metabeam is shown in Fig. 3(e), revealing the angular phase shifts between adjacent resonators in one cell. The time-domain signal that is sent to the high-voltage amplifier is a wide-band tone-burst excitation with a central frequency of 1500 Hz. For more details on the experimental setup, operation, and measurement synchronization, see the Supplemental Material and the accompanying video file [35]. Spatial and temporal Fourier transformations are performed on the SLDV velocity field data to extract the frequency content of propagating waves, and the result is then normalized by the excitation spectrum. By adopting a cantilever beam configuration with the ability to reverse the motor direction, we can effectively double the length of the beam without increasing the size of the structure: waves traveling from the piezoelectric actuator while the motors are rotating clockwise can be treated as waves traveling in the opposite direction while the motors are rotating counterclockwise. The metabeam is tested at two different modulation regimes, *quasistatic* and *dynamic*, based on the rotational speed of the motors, for both clockwise and counterclockwise rotations. The Supplemental Material video file demonstrates the apparatus in operation [35].

In the quasistatic modulation regime, the motors are rotated at a relatively low speed, 100 revolutions per minute (rpm) (1.67 Hz), compared to the natural frequencies of the resonators—which are higher than 1000 Hz. In addition, the resonators are oriented in a way to realize a spatially periodic variation of stiffness along the structure [similar to what is shown in Fig. 1(c)]. The combination of the spatial phase shift and the low-speed motor rotation generates space-time modulation of stiffness that slowly creeps along the metabeam. With a counterclockwise direction command, a backward modulation appears that is moving from the end to the root of the beam, while a clockwise command results in a forward modulation. This slow variation of stiffness is reminiscent of adiabatic pumping in quantum mechanical systems [36,37]. Despite the proven unconventional topological aspects of such systems [18,38], here we limit our attention to the spectral properties of the metabeam and dispersion characteristics rather than topological features of the modes. The metabeam is tested in both clockwise and counterclockwise rotations at 100 rpm and Fig. 4(a) illustrates the experimentally retrieved dispersion and transmission of the metabeam within the frequency range of interest, 600 to 3000 Hz. The right half-plane of the dispersion contours corresponds to the counterclockwise rotation and the left half-plane corresponds to the clockwise rotation,

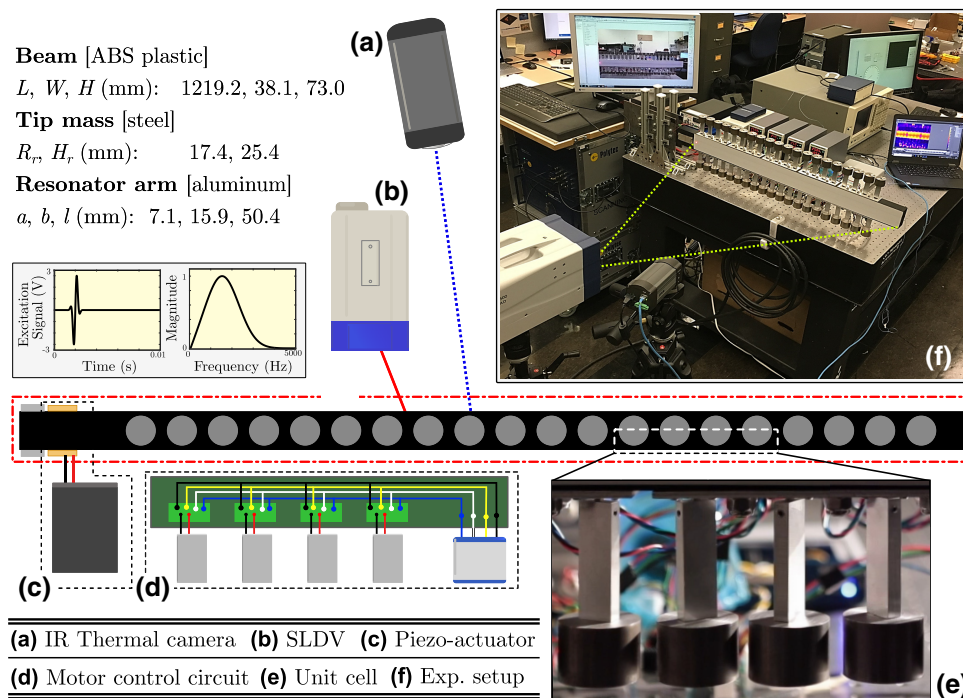


FIG. 3. Illustration of the complete experimental apparatus for the nonreciprocal elastic metabeam: (a) thermal imaging camera; (b) SLDV imaging system; (c) beam excitation module and the signal sent to the piezoelectric actuator; (d) power and controller circuit; (e) unit cell (bottom half, close-up); (f) and (g) metabeam.

which are shown along with their respective transmissions in Fig. 4(a). Note that the repeated flat lines in the dispersion plots (and alternating peaks in the spectra) are artifacts of the stepping frequency of the stepper motors that occurs at 200 times the rotational frequency (or 333.3 Hz); bipolar stepper motors with 1.8° advance per step impart both the main harmonic and 200 times its frequency. These lines are kept in the results to maintain originality and reproducibility of the data. Due to their reciprocal nature, the motor vibration artifacts do not interfere with our interpretation of the results, as they perfectly match in counterclockwise and clockwise dispersion patterns regardless of the modulation speed. From the close-up views in Figs. 4(b) and 4(c) we conclude that insignificant nonreciprocity between the forward and backward dispersion modes exists for this case. As intended, the traveling speed of the modulation (or the speed of motors) in the quasistatic modulation regime is insufficient to instigate detectable nonreciprocal response regardless of the rotational direction of the motors.

In the dynamic modulation regime, we intentionally increase the rotational speed of the motors to 2000 rpm (33.3 Hz) while maintaining the spatial modulation (angular position phase shift between the successive resonators). The result is a much faster traveling modulation and is shown in Fig. 4(d) along with the transmission spectra for both forward and backward modulations. As observed from the close-up views in Figs. 4(e) and 4(f), the faster modulation speed in the dynamic regime generated one-way modal transition and detectable nonreciprocal tilt of the dispersion modes. As a result,

the rightward-propagating branch is downshifted by an amount of 33.3 Hz (equal to the modulation speed, or rotational speed of motors) compared to the left propagating branch, which indicates the effectiveness of the proposed metabeam to break time-reversal symmetry. In accordance with the previous findings on reciprocity breakage in space-time modulated systems the frequency shift between the forward- and the backward-propagating branches is an integer multiple of the modulation frequency [38,39]. Accordingly, the nonreciprocity can be further accentuated by increasing the rotational speed of the motors. The one-way transmission at a given frequency can also be switched in the opposite direction by simply rotating motors in the opposite direction.

This work introduces an experimental realization of dynamically modulated metamaterials that do not rely on material response to external stimulus, but rather an inherent geometric attribute by design. A cornerstone feature of flexural materials, second area moment, is used to geometrically induce a space-time modulation and, consequently, enforce an artificial linear momentum bias to break time-reversal symmetry of waves in an elastic beam. It is experimentally demonstrated that nonreciprocal tilt of the dispersion modes is directly correlated with the modulation speed of the medium and can be adjusted all the way from complete reciprocal dispersion in the quasistatic regime to a complete nonreciprocal dispersion in the dynamic modulation regime. Nonreciprocal metamaterials can have extensive applications ranging from back scatter-free ultrasonic imaging and sensor-actuator protection to duplex underwater communications, SONAR

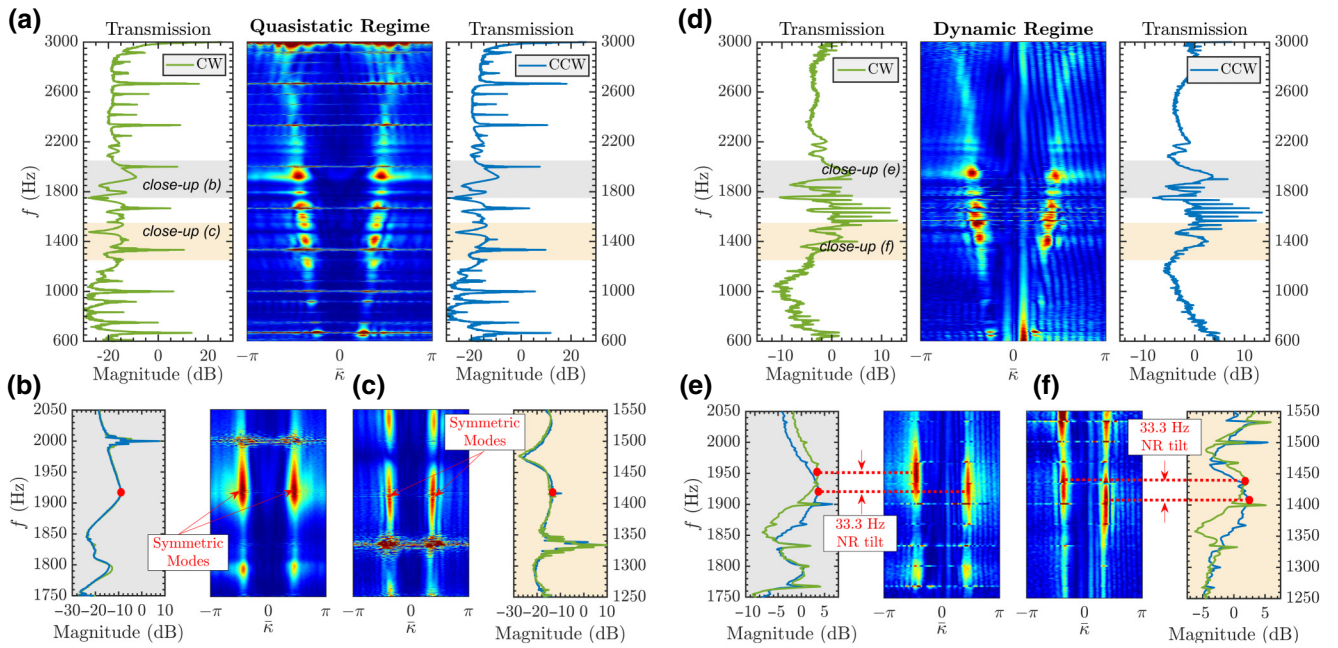


FIG. 4. Experimental results. (a) Quasistatic modulation regime with motors rotating at 100 rpm (1.67 Hz). Experimentally reconstructed dispersion patterns and transmission spectra obtained from backward [counterclockwise (CCW) rotation] and forward [clockwise (CW) rotation] modulated structures showing reciprocal response with fairly symmetrical counter-propagating modes due to low speed modulation. (b) Close-up: 1750–2050 Hz. (c) Close-up: 1250–1550 Hz. (d) Dynamic modulation regime with motors rotating at 2000 rpm (33.3 Hz). Experimentally reconstructed dispersion patterns and transmission spectra obtained from backward (counterclockwise) and forward (clockwise) modulated structures showing nonreciprocal tilt equal to the exact amount of the motors’ rotational speed for counter-propagating modes. (e) Close-up: 1750–2050 Hz. (f) Close-up: 1250–1550 Hz.

devices, and nonreciprocal acoustic phased array radars. Further, the current design also shows great potential to harbor topologically interesting features in future efforts. For instance, the quasistatic regime allows for adiabatic evolution of eigenstructure, which provides a realizable route to create topologically protected boundary modes in elastic structures.

ACKNOWLEDGMENT

The work was supported by the US National Science Foundation through Award No. 1847254 (CAREER), the Vibration Institute, as well as the New York State Center of Material Informatics.

[1] J. F. Doyle, in *Wave Propagation in Structures* (Springer, New York, USA, 1989), p. 126.
 [2] D. Mead, Wave propagation in continuous periodic structures: Research contributions from southampton, 1964–1995, *J. Sound Vib.* **190**, 495 (1996).
 [3] M. I. Hussein, M. J. Leamy, and M. Ruzzene, Dynamics of phononic materials and structures: Historical origins, recent progress, and future outlook, *Appl. Mech. Rev.* **66**, 040802 (2014).

[4] P. Celli and S. Gonella, Tunable directivity in metamaterials with reconfigurable cell symmetry, *Appl. Phys. Lett.* **106**, 091905 (2015).
 [5] Y. Chen, G. Huang, and C. Sun, Band gap control in an active elastic metamaterial with negative capacitance piezoelectric shunting, *J. Vib. Acoust.* **136**, 061008 (2014).
 [6] N. Swindeck, S. Matsuo, K. Runge, J. Vasseur, P. Lucas, and P. Deymier, Bulk elastic waves with unidirectional backscattering-immune topological states in a time-dependent superlattice, *J. Appl. Phys.* **118**, 063103 (2015).
 [7] H. H. Huang, C. T. Sun, and G. L. Huang, On the negative effective mass density in acoustic metamaterials, *Int. J. Eng. Sci.* **47**, 610 (2009).
 [8] M. B. Zanjani, A. R. Davoyan, A. M. Mahmoud, N. Engheta, and J. R. Lukes, One-way phonon isolation in acoustic waveguides, *Appl. Phys. Lett.* **104**, 081905 (2014).
 [9] R. Fleury, D. L. Sounas, C. F. Sieck, M. R. Haberman, and A. Alù, Sound isolation and giant linear nonreciprocity in a compact acoustic circulator, *Science* **343**, 516 (2014).
 [10] O. R. Bilal, A. Foehr, and C. Daraio, Bistable metamaterial for switching and cascading elastic vibrations, *Proc. Natl. Acad. Sci.* **114**, 4603 (2017).
 [11] M. A. Attarzadeh and M. Nouh, Elastic wave propagation in moving phononic crystals and correlations with stationary spatiotemporally modulated systems, *AIP Adv.* **8**, 105302 (2018).
 [12] A. Cullen, A travelling-wave parametric amplifier, *Nature* **181**, 332 (1958).

- [13] E. Cassedy and A. Oliner, Dispersion relations in time-space periodic media: Part I, stable interactions, *Proc. IEEE* **51**, 1342 (1963).
- [14] J. Achenbach, *Wave Propagation in Elastic Solids* (Elsevier, Amsterdam, The Netherlands, 2012), Vol. 16.
- [15] G. Trainiti and M. Ruzzene, Non-reciprocal elastic wave propagation in spatiotemporal periodic structures, *New J. Phys.* **18**, 083047 (2016).
- [16] M. A. Attarzadeh and M. Nouh, Non-reciprocal elastic wave propagation in 2d phononic membranes with spatiotemporally varying material properties, *J. Sound Vib.* **422**, 264 (2018).
- [17] E. Riva, J. Marconi, G. Cazzulani, and F. Braghin, Generalized plane wave expansion method for non-reciprocal discretely modulated waveguides, *J. Sound Vib.* **449**, 172 (2019).
- [18] M. A. Attarzadeh, H. Al Ba'ba'a, and M. Nouh, On the wave dispersion and non-reciprocal power flow in space-time traveling acoustic metamaterials, *Appl. Acoust.* **133**, 210 (2018).
- [19] H. Nassar, H. Chen, A. N. Norris, M. R. Haberman, and G. L. Huang, Non-reciprocal wave propagation in modulated elastic metamaterials, *Proc. R. Soc. A* **473**, 20170188 (2017).
- [20] H. Nassar, H. Chen, A. Norris, and G. Huang, Non-reciprocal flexural wave propagation in a modulated metabeam, *Extreme. Mech. Lett.* **15**, 97 (2017).
- [21] M. Ansari, M. Attarzadeh, M. Nouh, and M. A. Karami, Application of magnetoelastic materials in spatiotemporally modulated phononic crystals for nonreciprocal wave propagation, *Smart Mater. Struct.* **27**, 015030 (2017).
- [22] Y. Wang, B. Yousefzadeh, H. Chen, H. Nassar, G. Huang, and C. Daraio, Observation of Non-Reciprocal Wave Propagation in a Dynamic Phononic Lattice, *Phys. Rev. Lett.* **121**, 194301 (2018).
- [23] Y. Chen, X. Li, H. Nassar, A. N. Norris, C. Daraio, and G. Huang, Nonreciprocal Wave Propagation in a Continuum-based Metamaterial with Space-Time Modulated Resonators, *Phys. Rev. Appl.* **11**, 064052 (2019).
- [24] C. Croënne, J. Vasseur, O. Bou Matar, M.-F. Ponge, P. Deymier, A.-C. Hladky-Hennion, and B. Dubus, Brillouin scattering-like effect and non-reciprocal propagation of elastic waves due to spatio-temporal modulation of electrical boundary conditions in piezoelectric media, *Appl. Phys. Lett.* **110**, 061901 (2017).
- [25] G. Trainiti, Y. Xia, J. Marconi, G. Cazzulani, A. Erturk, and M. Ruzzene, Time-Periodic Stiffness Modulation in Elastic Metamaterials for Selective Wave Filtering: Theory and Experiment, *Phys. Rev. Lett.* **122**, 124301 (2019).
- [26] J. Marconi, E. Riva, M. Di Ronco, G. Cazzulani, F. Braghin, and M. Ruzzene, Experimental observation of non-reciprocal band-gaps in a space-time modulated beam using a shunted piezoelectric array, [arXiv:1909.13224](https://arxiv.org/abs/1909.13224) (2019).
- [27] S. P. Wallen and M. R. Haberman, Nonreciprocal wave phenomena in spring-mass chains with effective stiffness modulation induced by geometric nonlinearity, *Phys. Rev. E* **99**, 013001 (2019).
- [28] B. M. Goldsberry, S. P. Wallen, and M. R. Haberman, Non-reciprocal wave propagation in mechanically-modulated continuous elastic metamaterials, *J. Acoust. Soc. Am.* **146**, 782 (2019).
- [29] M. A. Attarzadeh, S. Maleki, J. L. Crassidis, and M. Nouh, Non-reciprocal wave phenomena in energy self-reliant gyric metamaterials, *J. Acoust. Soc. Am.* **146**, 789 (2019).
- [30] N. NejadSadeghi, L. Placidi, M. Romeo, and A. Misra, Frequency band gaps in dielectric granular metamaterials modulated by electric field, *Mech. Res. Commun.* **95**, 96 (2019).
- [31] N. NejadSadeghi and A. Misra, Axially moving materials with granular microstructure, *Int. J. Mech. Sci.* **161**, 105042 (2019).
- [32] X.-F. Lv, K.-C. Chuang, and A. Erturk, Tunable elastic metamaterials using rotatable coupled dual-beam resonators, *J. Appl. Phys.* **126**, 035107 (2019).
- [33] H. Sun, X. Du, and P. F. Pai, Theory of metamaterial beams for broadband vibration absorption, *J. Intell. Mater. Syst. Struct.* **21**, 1085 (2010).
- [34] H. B. Al Ba'ba'a and M. Nouh, Mechanics of longitudinal and flexural locally resonant elastic metamaterials using a structural power flow approach, *Int. J. Mech. Sci.* **122**, 341 (2017).
- [35] See Supplemental Material at <http://link.aps.org/supplemental/10.1103/PhysRevApplied.13.021001> for more details on the experimental setup, dispersion physics, and a video demonstration.
- [36] Y. E. Kraus, Y. Lahini, Z. Ringel, M. Verbin, and O. Zilberberg, Topological States and Adiabatic Pumping in Quasicrystals, *Phys. Rev. Lett.* **109**, 106402 (2012).
- [37] L. Wang, M. Troyer, and X. Dai, Topological Charge Pumping in a One-dimensional Optical Lattice, *Phys. Rev. Lett.* **111**, 026802 (2013).
- [38] R. Chaunsali, F. Li, and J. Yang, Stress wave isolation by purely mechanical topological phononic crystals, *Sci. Rep.* **6**, 30662 (2016).
- [39] H. Nassar, H. Chen, A. Norris, and G. Huang, Quantization of band tilting in modulated phononic crystals, *Phys. Rev. B* **97**, 014305 (2018).